

$$J_z \ddot{\psi} = \tau_z + \tau_d(t)$$

To express the yaw dynamics in standard state-space form, we define the state vector as

$$\mathbf{x} = \begin{bmatrix} \psi \\ r \end{bmatrix},$$

where ψ is the yaw angle and r is the yaw rate. The inputs to the system consist of the control yaw torque τ_z and an external disturbance torque τ_d , collected as

$$\mathbf{u} = \begin{bmatrix} \tau_z \\ \tau_d \end{bmatrix}.$$

Using these definitions and the linearized yaw equations

$$\dot{\psi} = r \text{ and } J_z \dot{r} = \tau_z + \tau_d,$$

the system, expressed in the linear form of $\dot{\mathbf{x}} = A\mathbf{x} + B\mathbf{u}$, is given by

$$\dot{\mathbf{x}} = \begin{bmatrix} \dot{\psi} \\ \dot{r} \end{bmatrix} = \begin{bmatrix} r \\ \frac{1}{J_z}(\tau_z + \tau_d) \end{bmatrix}.$$

The system matrices are

$$A = \begin{bmatrix} 0 & 1 \\ 0 & 0 \end{bmatrix}, \quad B = \begin{bmatrix} 0 & 0 \\ \frac{1}{J_z} & \frac{1}{J_z} \end{bmatrix}.$$

As the yaw angle and yaw rate are measured outputs, the output equation is given by $y = Cx + Du$ with

$$C = \begin{bmatrix} 1 & 0 \\ 0 & 1 \end{bmatrix}, \quad D = \begin{bmatrix} 0 & 0 \\ 0 & 0 \end{bmatrix}.$$

3 Transfer Functions and Block Diagrams

To develop a reliable yaw-control model for the quadcopter, we begin by examining its fundamental rotational dynamics. The yaw motion is governed by the moment of inertia J_z , which relates motor-generated torque to angular acceleration. Because yaw rate is the integral of angular acceleration and yaw angle is the integral of yaw rate, the plant behaves as a double integrator. When first designing the controller, a full PID controller was considered; however, the combination of the plant's inherent integral behavior and the additional integral term in the controller introduced significant difficulties. The system became more difficult to stabilize, accumulated excessive phase lag, and exhibited large overshoot. These issues resulted in us utilizing a PD controller instead, which retains the proportional correction and provides needed

damping through the derivative term without further destabilizing the dynamics. The resulting block diagram reflects this more stable and practical control approach.

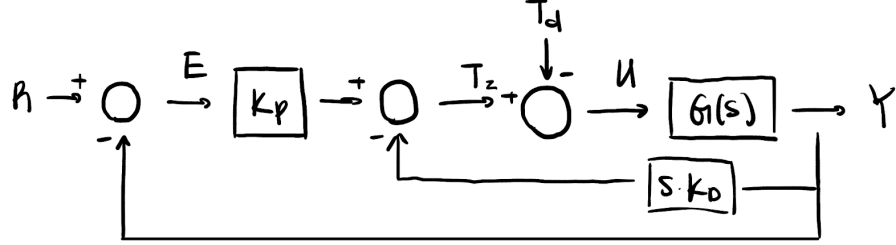


Figure 3. Block Diagram

$$G(s) = \frac{1}{J_z s^2}$$

$$\frac{Y(s)}{R(s)} = \frac{K_p}{J_z s^2 + K_D s + K_p}$$

The two state variables ψ and r describe the quadcopter's yaw orientation and its yaw rate, respectively. These states change according to the torque applied by the motors, which serves as the control input. The transfer function $G(s) = \frac{1}{J_z s^2}$ reflects the relationship between this input torque and the resulting yaw motion: applying torque changes angular acceleration, which affects yaw rate, and ultimately alters the yaw angle. Within the PD controller, the reference yaw angle is continuously compared with the current yaw angle, and the resulting error determines the corrective torque. The proportional term addresses immediate angle error, while the derivative term reacts to the yaw rate, adding damping that helps reduce overshoot and stabilize the response. This structure ensures that the quadcopter can accurately follow yaw commands while remaining robust to disturbances and variations in operating conditions.

4 Active Control

As outlined above, we decided to use a PD control structure. We started with the dynamics in the Laplace domain, as:

$$J_z s^2 \Psi(s) = T_z(s)$$

From the dynamics above, we implemented our PD control law, as

$T_z(s) = K_P(\Psi_{\text{ref}}(s) - \Psi(s)) - K_D s \Psi(s)$. We only have a $\Psi(s)$ term on K_D , as our desired velocity is zero. We are able to rearrange our original dynamics equation above to find our closed loop transfer function:

$$H(s) = \frac{\Psi(s)}{\Psi_{\text{ref}}(s)} = \frac{K_P}{J_z s^2 + K_D s + K_P}$$

Now, we know that the maximum torque for this system is 34 Nm, and with a desired step size from 0 to π , we know that our K_P value to achieve this must be:

$$\tau_{\text{initial}} = K_P e_{\max} \implies K_P = \frac{34 \text{Nm}}{\pi \text{ rad}} \approx 11$$

To find K_D , we first need to find the system's natural frequency. Since the poles of this system are in general second order form, we can rewrite the K_P term as ω_n^2 . This means that after normalizing, we find that:

$$\omega_n = \sqrt{\frac{K_P}{J_z}} \implies \omega_n = \sqrt{\frac{11}{69}} \approx 0.40 \text{ rad/s}$$

Now, we can rewrite the $K_D s$ term as the second order analogue of $2\zeta\omega_n$. We want our system to be critically damped ($\zeta = 1$), so writing out the parameter in normalized form:

$$\frac{K_D}{J_z} = 2\zeta\omega_n \implies K_D = 2J_z\zeta\omega_n \implies K_D \approx 55$$

This means that for the loaded case, we get $K_P = 11$ and $K_D = 55$. For the unloaded case, we can repeat the same derivation process with the unloaded inertia value of $J_z = 31 \text{ kg m}^2$, and get $K_P = 11$ and $K_D = 37$.

5 Bode Plot Analysis

To better understand how the yaw-control system behaves in real flight conditions, Bode plots were generated for both the loaded and unloaded configurations of the aircraft. Because the yaw dynamics behave like a double integrator, the system's performance is largely shaped by a pair of dominant poles associated with the vehicle's rotational inertia. These poles determine how quickly the vehicle can respond and how much phase lag it accumulates as frequency increases. The following will analyze each plot individually and compare how payload-induced changes in inertia influence overall stability and responsiveness.

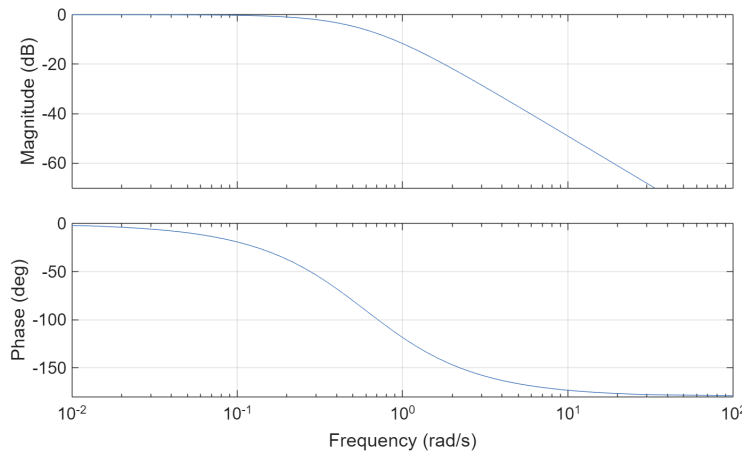


Figure 4. BAE/Malloy T150 Heavy Lift UAS Yaw Control Bode Plot (Unloaded)

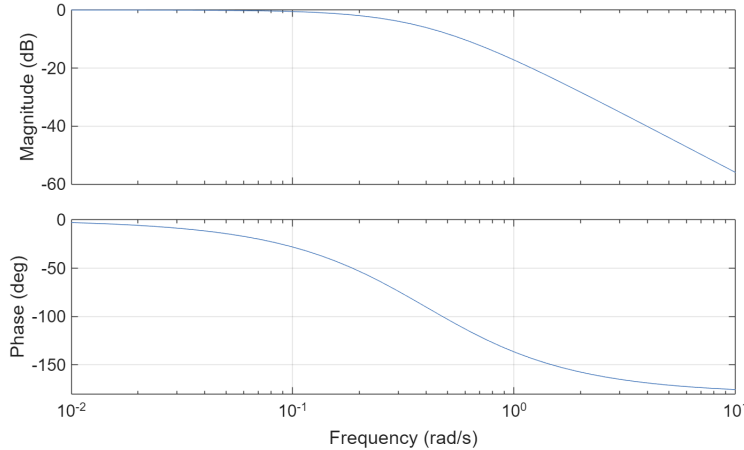


Figure 5. BAE/Malloy T150 Heavy Lift UAS Yaw Control Bode Plot (Loaded)

A comparison of the unloaded and loaded yaw-control responses shown in Figures 3 and 4 demonstrates how increasing the rotational inertia slows the dynamic response and reduces the bandwidth. In the unloaded case (Figure 4), the aircraft has a lower rotational inertia of $J_z = 31\text{kgm}^3$, combined with $K_p = 11$ and a derivative gain of $K_d = 37$. The system achieves the same magnitude at a higher frequency and a more gradual magnitude roll-off in comparison to the loaded case, indicating the yaw control responds more quickly and has a wider bandwidth. This occurs because the lower inertia allows the dominant poles of the double-integrator plant to remain at higher frequencies, enabling faster yaw response and more gradual phase decay.

In contrast, the loaded configuration (Figure 5) increases the inertia to $J_z = 69\text{kgm}^3$, requiring a larger derivative gain of $K_d = 55$ to counteract the greater phase lag introduced by the added payload. Both the magnitude and phase curves are shifted leftward, showing that the system begins losing gain and phase margin at lower frequencies. Even with a higher K_d value, the loaded response exhibits an earlier magnitude roll off and the phase approaches -180° at a lower frequency, indicating a narrower bandwidth and slower dynamic response.

Overall, Figures 4 and 5 show that the unloaded aircraft is naturally more agile, while the loaded configuration trades some responsiveness for stability under higher inertia.